A comparative study of Rayleigh-Taylor and Richtmyer-Meshkov instabilities in 2D and 3D in tantalum

Z. Sternberger, B. R. Maddox, Y. P. Opachich, C. E. Wehrenberg, R. G. Kraus, B. A. Remington, G. C. Randall, M. Farrell, and G. Ravichandran

Citation: **1793**, 110006 (2017); doi: 10.1063/1.4971669

View online: http://dx.doi.org/10.1063/1.4971669

View Table of Contents: http://aip.scitation.org/toc/apc/1793/1

Published by the American Institute of Physics

A Comparative Study of Rayleigh-Taylor and Richtmyer-Meshkov Instabilities in 2D and 3D in Tantalum

Z. Sternberger[1], B. R. Maddox[2], Y. P. Opachich[3], C. E. Wehrenberg[2], R. G. Kraus[2], B. A. Remington[2], G. C. Randall[4], M. Farrell[4] and G. Ravichandran[1]

[1]*California Institute of Technology, Pasadena, CA 91125, USA*
[2]*Lawrence Livermore National Laboratory, Livermore, CA 94551, USA*
[3]*National Security Technologies, LLC, Livermore, CA 94551, USA*
[4]*General Atomics, San Diego, CA 92121, USA*

Abstract. Driving a shock wave through the interface between two materials with different densities can result in the Richtmyer-Meshkov or Rayleigh-Taylor instability and initial perturbations at the interface will grow. If the shock wave is sufficiently strong, the instability will lead to plastic flow at the interface. Material strength will reduce the amount of plastic flow and suppress growth. While such instabilities have been investigated in 2D, no studies of this phenomena have been performed in 3D on materials with strength.

Initial perturbations to seed the hydrodynamic instability were coined into tantalum recovery targets. Two types of perturbations were used, two dimensional (2D) perturbations (hill and valley) and three-dimensional (3D) perturbations (egg crate pattern). The targets were subjected to dynamic loading using the Janus laser at the Jupiter Laser Facility. Shock pressures ranged from 50 GPa up to 150 GPa and were calibrated using VISAR drive targets.

INTRODUCTION

The classic Rayleigh-Taylor instability (RTI) example begins with two fluids of different densities. The interface between the fluids is given a small sinusoidal perturbation and then the light fluid is accelerated into the heavy fluid, normal to the interface, causing the amplitude of the interface to grow. A linearized analysis with $\eta k \ll 1$ shows the amplitude of the initial perturbation grows according to,

$$\eta = \eta_0 e^{\sqrt{gkAt}} \tag{1}$$

where η is the interface amplitude, g is the acceleration, k is the wave number of the perturbation, and A is the Atwood number [1]. In the case of an impulsive loading of the interface, such as a shock passage, the interface initially grows according to the Richtmyer-Meshkov instability (RMI),

$$\eta = A\eta_0 kUt + \eta_0 \tag{2}$$

where U is the interface velocity imparted by the passage of the shock [2].

The dimensionality of the initial perturbation, whether 2D (hills and valleys) or 3D (egg crate pattern), affects the growth rate of the instability. In fluids, 3D initial perturbations with a wave number $k = \sqrt{k_x + k_y}$ have been shown to grow more than 2D initial perturbations with the same wave number [3].

The physics of the problem can be altered by replacing the denser fluid with a solid. In order for the initial perturbation to grow, the interface must be driven sufficiently to overcome the strength of the solid. An analytic model of the RMI of a solid-gas interface by Piriz et al. [4] shows that the growth of the amplitude is inversely proportional to the yield strength of the material. The strength of a material can then be inferred by its resistance to instability. Mikaelian has modeled the reduction of instability growth by introducing viscosity. A correspondence between viscosity and strength can then be used to relate the instability growth to strength [5, 6].

Shock Compression of Condensed Matter - 2015
AIP Conf. Proc. 1793, 110006-1–110006-4; doi: 10.1063/1.4971669
Published by AIP Publishing. 978-0-7354-1457-0/$30.00

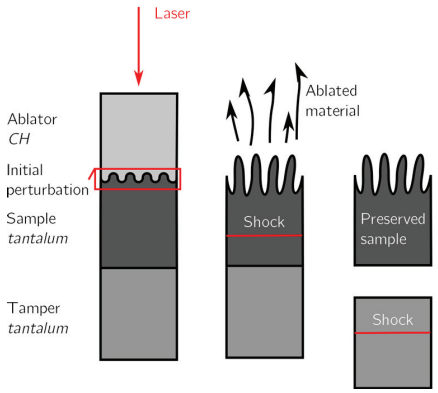

FIGURE 1. On the left, the laser strikes the target and starts to ablate the ablator. The shock enters the target and the ripples grow due to RMI. On the right, the shock enters the tamper and the target is recovered.

Park et al. have performed RTI experiments in tantalum [7, 8]. A tantalum foil is ramp accelerated by the release of laser ablation products and in flight radiography tracks the growth of the 2D initial perturbations. The strength of the tantalum evolves under the extreme pressures (100 GPa) and strain rates (10^7 s^{-1}) and increases the material's resistance to instability.

Prime et al. have performed RMI experiments in copper [9]. A shock propagates through a copper sample and releases at the rear surface, achieving strain rates on the order of 10^6 s^{-1}. Initial perturbations on the rear surface grow under RMI. For some initial perturbations, strength arrests the growth of the initial perturbation.

As the addition of material strength affects the classical instability growth rates, strength may also affect the influence of initial perturbation dimensionality. Results from Lebedev et al. [10] indicate that in a solid-gas system, 2D initial perturbations grow more than 3D initial perturbations. The initial perturbations were driven by explosion products releasing over a vacuum gap. The resulting ramp loading drives growth due to RTI.

The following work considers the case of shock loading and perturbation growth due to RMI in tantalum targets.

EXPERIMENTAL DESIGN

Two initial perturbation patterns are used, one 2D and one 3D, with $\lambda_x = \lambda_y = 100$ μm for the 3D perturbation and $\lambda = 50$ μm for the 2D perturbation. The amplitude of both patterns is $\eta_0 = 5$ μm. The patterns are diamond turned into steel dies which are used to coin the pattern onto 3 mm diameter tantalum disks [11]. A fiducial is imprinted on each target.

The amplitude of the coined surface varies slightly over the surface of the disc. The coined surface is profiled with interferometry to record the initial perturbation amplitudes. A 220 μm polystyrene ablator is glued to the coined disc to couple the laser energy to the target. A large tamper is glued to the back of the target as a momentum trap to prevent damage to the target. The targets are driven by a 3 ns square pulse of 527 nm light at the Janus laser at the Jupiter Laser Facility. The laser was focused to either a 1 mm^2 spot or a smaller 0.3 mm^2 spot to increase laser intensity. Hyades, a 1D laser ablation code [12] was used to select a range of laser energies (100-400 J) to produce a range of shock pressures around 100 GPa.

VISAR [13] results from drive targets show laser ablation of the target produces a blast wave. The passage of the shock wave causes growth due to RMI. The release following the initial shock accelerates the heavy tantalum into the light polystyrene, causing Rayleigh-Taylor dynamics with a negative Atwood number. Consequently, the interface stops growing and begins to oscillate back towards its initial amplitude. After some time, the release will weaken to a point where it no longer causes plastic flow and the evolution of the amplitude ceases. This final recovered amplitude is therefore a product of two hydrodynamic instability dynamics.

Peak interface pressure is calibrated to laser energy using a series of VISAR drive targets that span the range of laser energies and a Hugoniot for tantalum [14]. The drive achieved a range of peak pressures at the polystyrene and tantalum interface pressures from 50 GPa to 150 GPa.

After the experiment, the tantalum disks are recovered, cleaned of ablator debris, and profiled with interferometry

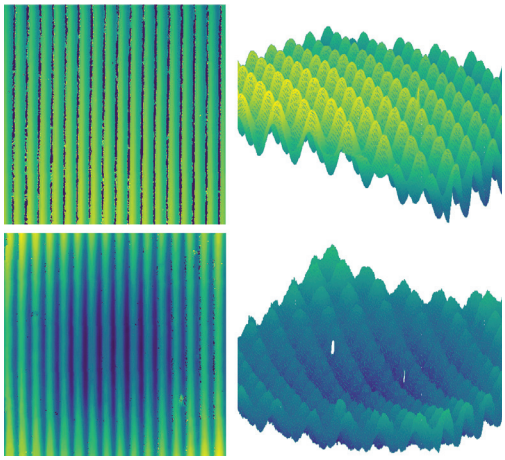

FIGURE 2. Example profiles of 2D (left) and 3D (right) targets. Blue regions are deeper than the green regions. The top profiles are recorded before the laser drive with $\eta_0 = 5\ \mu$m. The bottom are recorded after the drive and show a prominent depression in the profile from the laser drive. The 3D profile amplitudes are exaggerated relative to the wavelength.

(Figure 2). The fiducial survives the experiment, allowing a profile after the experiment to be compared to the original profile. The most prominent feature in the profiles is the depression caused by the drive. The deepest part of this depression is defined as the shot center. The amplitudes that lie within a 300 μm radius of the shot center are averaged. The same average is calculated over the original amplitudes and the ratio of the average amplitude after to the average amplitude before is defined as the growth factor.

RESULTS

From the averaged profiles and the VISAR calibration, instability growth can be compared over a range of peak pressures at the rippled interface, Figure 3. As peak pressure increases to around 100 GPa, the recovered growth factor increases to a maximum of roughly 1.4. Increases in peak pressure above 120 GPa decrease the recovered growth factor in both the 2D and the 3D targets. We suspect this behavior is caused by a stronger release wave undoing the growth caused by RMI. The recovered target perturbations are roughly sinusoidal for all drive pressures without the classic mushroom shape that develops in nonlinear instability growth.

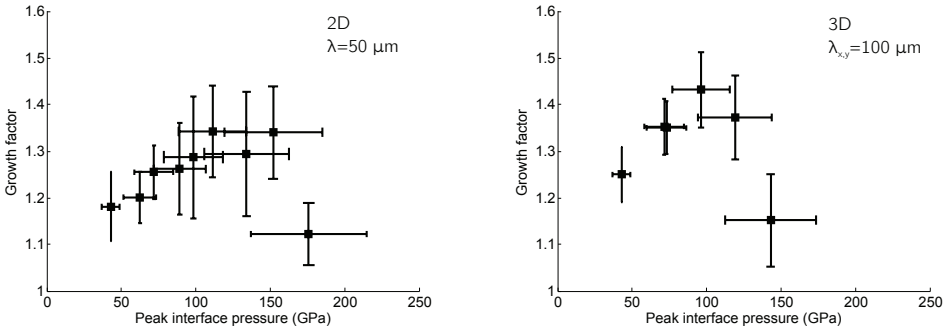

FIGURE 3. Recovered ripple growth in 2D targets (left) and 3D targets (right) as a function of the peak pressure at the interface.

The amplitudes near the shot center are not uniform, contributing to the uncertainty in growth factor. In 2D and 3D targets, variation in recovered amplitude increases with increasing peak pressure up to 100 GPa. The uncertainty in peak interface pressure is set by variations between the breakout velocities measured with VISAR in drive targets.

Ideally, the 2D and 3D wave numbers would be the same so that the initial RMI growth rate is the same for each perturbation. As the 2D and 3D perturbation wave numbers are different in this experiment, the instability behavior is

different. The 3D perturbations grow slower than the 2D perturbations immediately after the shock. Because of this complication and because the recovered growth factor is due to the combined effects of RTI and RMI, it is difficult to interpret the results without understanding the time evolution of the interface. Planned simulations of the interface will help untangle the competing effects of the shock and the release wave.

In summary, we have successfully shock loaded and recovered 2D and 3D ripple samples over a wide range of pressures. These samples exhibit complex fluid instabilities that will be useful for benchmarking future hydrocode simulations and strength models at high strain rates.

ACKNOWLEDGMENTS

The authors would like to thank the staff at the Jupiter Laser Facility at Lawrence Livermore National Laboratory for their help during our experimental campaign. This work was completed with the support of the NNSA through the HEDLP program, grant numbers DE-NA0001805 and DE-NA0001832.

REFERENCES

[1] G. Taylor, Proceedings of the Royal Society of London A: Mathematical, Physical and Engineering Sciences **201**, 192–196 (1950).
[2] R. D. Richtmyer, Communications on Pure and Applied Mathematics **13**, 297–319 (1960).
[3] M. M. Marinak, B. A. Remington, S. V. Weber, R. E. Tipton, S. W. Haan, K. S. Budil, O. L. Landen, J. D. Kilkenny, and R. Wallace, Physical Review Letters **75**, 3677–3680 (1995).
[4] A. R. Piriz, J. J. Lopez Cela, N. A. Tahir, and D. H. H. Hoffmann, Physical Review E **78**, p. 056401 (2008).
[5] K. O. Mikaelian, Physical Review E **47**, 375–383 (1993).
[6] K. O. Mikaelian, Physical Review E **87**, p. 031003 (2013).
[7] H.-S. Park, N. Barton, J. L. Belof, K. J. M. Blobaum, R. M. Cavallo, A. J. Comley, B. Maddox, M. J. May, S. M. Pollaine, S. T. Prisbrey, B. Remington, R. E. Rudd, D. W. Swift, R. J. Wallace, M. J. Wilson, A. Nikroo, and E. Giraldez, "Experimental results of tantalum material strength at high pressure and high strain rate," in *AIP Conference Proceedings*, Vol. 1426 (2012), pp. 1371–1374.
[8] H.-S. Park, R. Rudd, R. Cavallo, N. Barton, A. Arsenlis, J. Belof, K. Blobaum, B. El-dasher, J. Florando, C. Huntington, B. Maddox, M. May, C. Plechaty, S. Prisbrey, B. Remington, R. Wallace, C. Wehrenberg, M. Wilson, A. Comley, E. Giraldez, A. Nikroo, M. Farrell, G. Randall, and G. Gray, Physical Review Letters **114**, p. 065502 (2015).
[9] M. B. Prime, W. T. Buttler, S. K. Sjue, B. J. Jensen, F. G. Mariam, D. M. Or, C. L. Pack, J. B. Stone, D. Tupa, and W. Vogan-McNeil, in *Dynamic Behavior of Materials, Volume 1*, Conference Proceedings of the Society for Experimental Mechanics Series (2016), pp. 191–197.
[10] A. Lebedev, P. N. Nizovtsev, V. Raevskii, and V. P. Solov'ev, Physics - Doklady **41**, 328–330 (1996).
[11] G. C. Randall, J. Vecchio, J. Knipping, D. Wall, T. Remington, P. Fitzsimmons, M. Vu, E. M. Giraldez, B. E. Blue, M. Farrell, and A. Nikroo, Fusion Science and Technology **63**, 274–281 (2013).
[12] J. T. Larsen and S. M. Lane, Journal of Quantitative Spectroscopy and Radiative Transfer **51**, 179–186 (1994).
[13] L. M. Barker and R. E. Hollenbach, Journal of Applied Physics **43**, 4669–4675 (1972).
[14] S. P. Marsh, *LASL shock Hugoniot data*, Vol. 5 (Univ of California Press, 1980).